Peak pressure and contact profile during sideways falls on the hip: links with individual characteristics and falling configuration

I.C. Levine and A.C. Laing
Department of Kinesiology, University of Waterloo, Waterloo, ON

ABSTRACT

Characterization of load distribution in the floor-pelvis contact plane during a fall may improve prediction of hip fracture risk, protective equipment design, and identification of "high-risk" falling configurations. Further, while estimation of the forces applied tothe hip during a fall can be achieved through multi-body modeling, Hertzian and volumetric contact models assume circular contact profiles. No published literature has linked falling configuration or soft tissue thickness (STT) with peak pressure or contact profile. The objective of this study was to test the hypotheses that (1) peak pressure would be greater in males and low-STT participants, as well as during fall simulation protocols (FSP: "Pelvis Release", "Kneeling Release" and "Squat Release") with less hip flexion; (2a) overall contact area and Harmonic 0 (mean radius) would be lower in males and low-STT participants, but similar between FSP; (2b)) the Pelvis Release protocol would produce contact profiles most circular in shape; (3) contact profile elements would negatively correlate with peak pressure. Forty-four young, healthy participants (23 female) consented to undergo an eighteen-trial protocol. STT was measured via ultrasound. Peak pressure, contact area and ellipse descriptors were quantified at time of peak pressure. No pressure or contact profile variable differed significantly between males and females. Peak pressure ranged from 307-9992 kPa, and differed between FSP. Contact Area and Harmonic 0 were lower for low-STT fallers, and lower during Pelvis Release. Contact profiles differed between STT-groups and FSP, and 76.1% of trials had contact profiles with eccentricity greater than 2.0. Peak pressure was negatively correlated with ellipse descriptors only during Pelvis Release. To summarize, peak pressure varied substantially only between falling configurations. However, contact profile characteristics were linked with peak pressure; unexplored individual characteristics or falling kinematics may drive these variables. Finally, contact profiles were substantially "round", but more work should examine the sensitivity of load prediction models to more complex contact profiles.

INTRODUCTION

The primary theory linking trochanteric soft tissues with hip fracture suggests that fracture risk is reduced through energy absorption by the soft tissues (Cummings and Nevitt, 1994; Etheridge, 2005; Hayes, 1996), with magnitude of absorption dependent on soft tissue thickness (STT) (Robinovitch, 1995b). This theory is linked to lower epidemiological risk of fracture in high-BMI fallers (Johansson, 2014). Mechanistically, however, soft tissue thickness is predictive of fracture risk in women (Bouxsein, 2007) but not men (Nielson, 2009), though expected force,

attenuated by soft tissue, was lower for controls than fracture cases in both studies. Further, despite noted difference in STT between sexes (Levine, 2014), and positive correlation between body mass index (BMI) and STT (Levine, 2014; Robinovitch, 1991), energy absorption during a lateral hip impact differs between BMI groups but not sexes (Bhan 2014). Additionally, estimates of pelvic system stiffness differ between sexes but not BMI groups (Levine, 2013). These inconsistencies highlight the need for further investigation of the mechanisms governing STT reduction of hip fracture risk.

The relationship between STT and reduction of load at the hip may be more complex than absorption of energy through one-dimensional compression. First, quantity of STT is not stagnant: apparent STT increases with degree of hip flexion (Levine, 2014), which would be reflected during falling configurations with differing magnitude of hip flexion. Second, soft tissue distribution of loads, i.e. pressure and contact profile, may be equally important as absorption. This more robust theory supports the design of hip protectors (Robinovitch, 2009, 1995a) and safety floors (Laing, 2006). Third, the majority of fall simulation protocols used to characterize impact dynamics are constrained to one axis (within the transverse plane of the pelvis); real-life falls comprise substantial non-vertical velocity and loading components. Better understanding of the three-dimensional nature of load distribution may improve prediction of hip fracture risk, protective equipment design, and identification of "high-risk" falling configurations. Therefore, pressure (loading localized at the "danger zone" directly overlying the proximal femur (Choi, 2010a, 2010b)), or contact area (a measure of the distribution of loads) may improve prediction of hip fracture risk.

While rapid estimation of the forces applied to, and distributed between body segments during a fall can be achieved through multi-body modeling, Hertzian and volumetric contact models (Boos and McPhee, 2013; Gonthier, 2005) assume circular contact. Characterization of model parameters requires experimental data conforming to the force distribution assumptions. However, thigh contact during a simulated fall could increase the geometric eccentricity (deviation from circular) of the contact profile. It is unknown whether contact profiles during sideways falls impacting the hip are suitably 'circular' to characterize stiffness and damping parameters for such models.

Radial Fourier Analysis is a morphometric method using semilandmarks (a sequence of equiangular minor landmarks which define a curve) to quantify the shape of a two-dimensional outline such as a contact profile (Ehrlich and Weinberg, 1970). The method is commonly used in paleontology to discriminate species based on shape (Lohmann, 1983). The polar coordinates of the shape are analyzed to determine the primary elements which interfere to produce the curve, with harmonic number (H1…H*n*) indicating the number of lobes (circle=1, ellipse=2, trilobe=3…) and harmonic amplitude indicating the relative contribution of that lobe to the composite shape. Harmonic 0 quantifies the mean radius of the shape, and can be used to normalize the amplitude of H1…H*n.* Therefore, the analysis method can be both sensitive to, and independent of scale. In the context of contact profiles, H0 would be interpreted as a metric related to contact area, H1 would reflect the size of the circular portion of the contact profile, while H2 would indicate the elliptical shape of the contact profile, reflecting distal thigh contact. In contrast, eccentricity simply quantifies the elliptical component. However, these approaches have never been used to characterize contact profiles during lateral impacts with humans. It is also unclear whether Radial

Fourier Analysis provides more relevant data regarding pressure distribution than simple eccentricity.

The primary objective of this study was to quantify differences in a) peak pressure, and b) contact profile, between sexes, STT group and fall simulation method, during simulated fall protocols designed to constrain or incorporate realistic falling characteristics. The second objective was to link changes in contact profile with peak pressure. We hypothesized that (1) peak pressure would be greater in males (compared to females) and low-STT participants (compared to mid- or high-STT participants), as well as during fall simulation protocols (FSP) with less hip flexion (i.e impact configurations with reduced available STT). Regarding contact profile, we hypothesized that (2a) indices of contact area would be lower in males (compared to females) and low-STT participants (compared to mid- or high-STT participants), but similar between FSP; (2b) the Pelvis Release protocol would produce contact profiles most circular in shape. Finally, we hypothesized that (3) contact profile elements would negatively correlate with peak pressure.

METHODS

Forty-four healthy participants (<35 years, 23 female) consented to participate in this study (Table 1). Participant recruitment focused on developing a cohort with a wide variety of body composition. Exclusion criteria included musculoskeletal injury in the past year preventing completion of the protocol, lifetime fracture history, fear of falling, or other health conditions which would make participation unsafe. Transverse-plane STT was assessed via ultrasound (C60x, 2-5 MHz transducer, M-Turbo Ultrasound, SonoSite, Inc., Bothell, WA) in a side-lying position, similar to that expected during the impact phase of the fall simulations**.** Participants were grouped into low-, mid- and high-STT groups based the following criteria: males low <3, mid 3.1-4, high >4.1 cm; females low <3.5, mid 3.6-5, high >5 cm. These thresholds represent low- (<18.5 kg/m^2), moderate (18.6-25 kg/m^2) and high- (>25.1 kg/m^2) BMI older adults (unpublished data).

Table 1: Mean (SD) participant anthropometric characteristics. STT represents trochanteric soft tissue thickness. BMI represents body mass index

		N	Height (m)	Mass (kg)	BMI (kg/m^2)	STT (cm)
Females						
STT	Low	7	1.62 (0.04)	54.0 (6.1)	20.4 (1.7)	3.0 (0.4)
	Mid	9	1.66 (0.06)	64.6 (10.3)	23.2 (2.8)	4.3 (0.4)
	High	7	1.66 (0.07)	85.8 (20.6)	31.5 (7.9)	6.9 (2.0)
Males						
STT	Low	8	1.80 (0.07)	72.5 (11.5)	22.4 (2.3)	2.3 (0.5)
	Mid	7	1.79 (0.08)	83.4 (10.9)	26.1 (3.2)	3.5 (0.5)
	High	6	1.77 (0.02)	92.1 (9.7)	28.7 (2.9)	4.9 (0.3)

Experimental Protocol

An eighteen-trial fall simulation protocol (FSP) consisted of six blocks of trials, each block consisting of one Pelvis Release, one Kneeling Release and one Squat Release protocol (Figure 1), in randomized order. Blocks 1-3 were "training trials", allowing for participant adaptation to the protocol; Blocks 4-6 were used to determine biomechanical outcomes. All paradigms involved the lateral aspect of the left hip impacting a pressure plate (4096 resistive sensors, each 0.762 by 0.508 cm, 500 Hz; FootScan, RSScan, Olen, Belgium) overlying a force plate (3500 Hz; OR6-3, AMTI, USA). The force and pressure plates were spatially aligned and temporally synchronized using a motion capture system (Optotrak Certus, Northern Digital, Inc., Waterloo, ON).

The primary difference between the protocols is the motion path of the pelvis: a controlled, vertical motion is produced during Pelvis Release, while Kneeling Release produces vertical and lateral motion in an inverted pendulum, and Squat Release typically has more lateral than vertical motion. For the Pelvis Release, the upper body of the participant was supported by a pillow outside the contact area of the force plate. For the Kneeling Release and Squat Release, the participant held a pillow throughout the trial to prevent bracing with their arms during the impact. The Pelvis Release protocol is highly controlled, and represents a scenario where the faller rotates into a horizontal position before impacting the hip directly laterally. The Kneeling Release reflects a scenario where the faller impacts the knee prior to rotating to impact the hip. The Squat release reflects a scenario where the faller flexes the knee, hip and ankle during the descent phase prior to rotating laterally to impact the hip.

In greater detail, for the initial position for Pelvis Release, hips were flexed to 45°, knees were flexed to 90°, and the pelvis was raised in a thin nylon sling using a turnbuckle until the soft tissues overlying the hip were 5 cm above the pressure plate. The participant was instructed to reduce the muscle tension in their body; when the participant reported that they were "relaxed and ready", the electromagnet supporting the sling was released, allowing the pelvis of the participant to impact the pressure plate. For Kneeling and Squat Release, the participant was supported in the initial position by the researcher, was instructed to lean until their weight was supported by their left side, self-release, and fall "like a pendulum". For kneeling release, the initial position was hips were flexed to 0°, knees were flexed to 90° and the lower leg was in contact with the starting mat. For Squat Release the initial position was a heel-lifted Squat, with maximal thigh-calf contact and

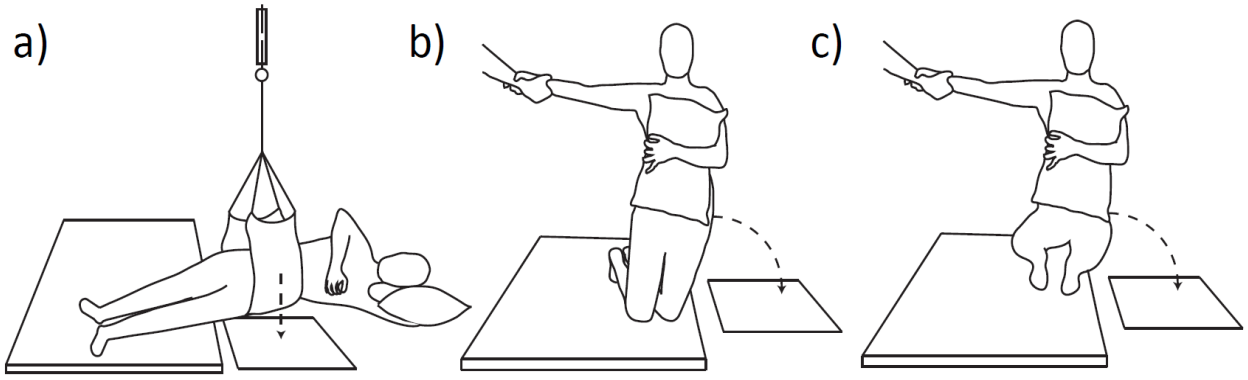

Figure 1: Initial position and motion path of the Pelvis Release (a), Kneeling Release (b), and Squat Release (c).

an upright torso. Mean (SD) hip flexion angles for Pelvis, Kneeling and Squat release were 50.9 (28.6)°, 34.7 (20.0)° and 76.3 (13.2)°, respectively. A minimum of one minute of rest was provided between each trial, during which the participant was asked to stand or kneel without contact between the ground and trochanteric or gluteal soft tissues.

Signal Processing

Data processing employed customized MATLAB routines (MathWorks, Natick, MA). Peak pressure magnitude (P_{peak}) was determined as the sensel with the greatest magnitude; associated location and time were also extracted. The contact profile (CP) associated with P_{peak_time} was further processed: first the CP was converted to a binary matrix, and an iterative algorithm was used to include active sensels within a three-sensel radius of sensels concurrent with $P_{peak\_location}$ at P_{peak_time}. The final CP was used to mask distal and proximal body segment contacts to determine Contact Area (*CA*). Polar coordinates (relative to $P_{peak\_location}$) were determined for the outermost sensels in the CP (Figure 2). The resulting waveform was resampled to produce a minimum of 100 samples between 0 and 2π. Major axis (*M*) was identified as the wafeform maximum; minor axis (m) was the minimum of the data located $+\pi/2$ and $-\pi/2$ radians from *M*.

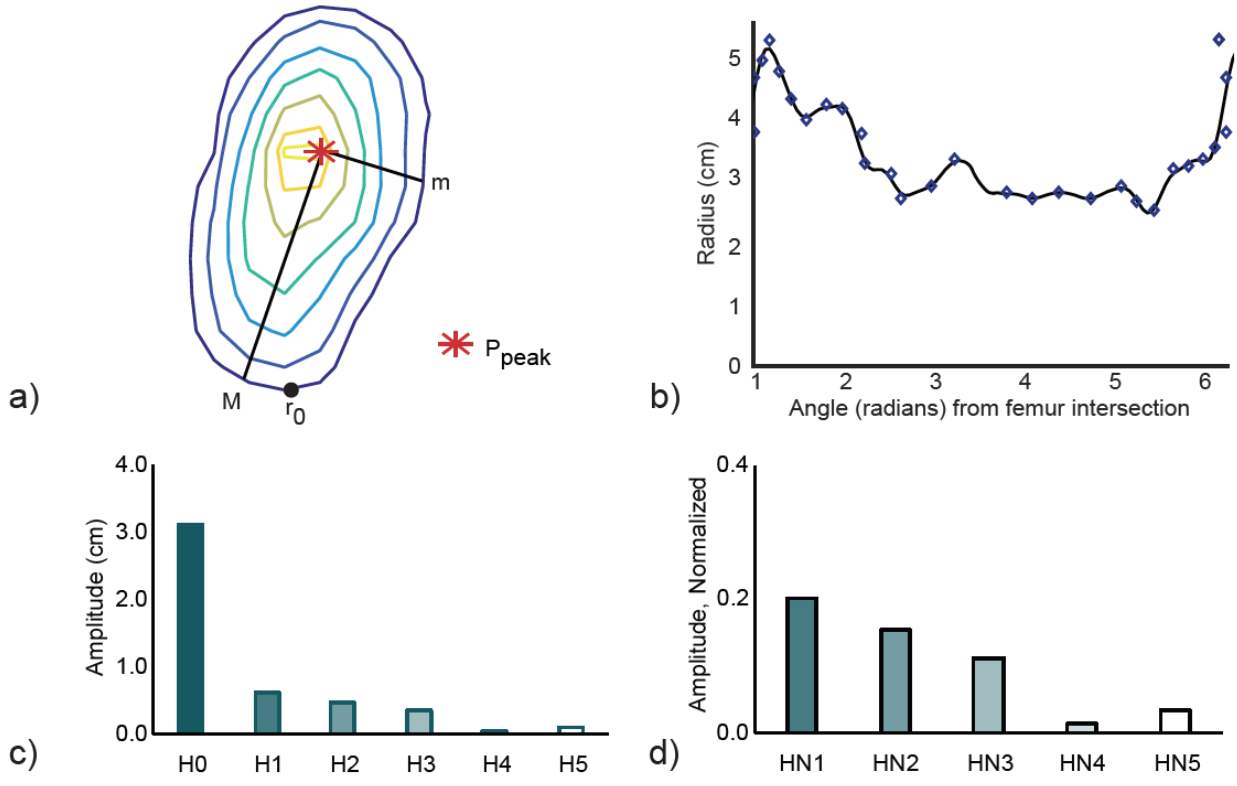

Figure 2: Analysis of the floor-pelvis contact profile. The perimeter of the contact area (indigo line, a) is used to develop a waveform (b). Beginning at the femur intersection point (r_0), radii are determined, including major axis (M) and minor axis (m). The waveform is analyzed to produce harmonic amplitudes (c) and normalized harmonic amplitudes (d).

Eccentricity was calculated as *M/m*. Fourier analysis on the repeated waveform generated mean radius (*H0*) and amplitude of *H1…H5*. Harmonics one through four were also normalized to *H0* (*HN1…HN5*) to determine the relative amplitude of each harmonic.

Data Analysis

Statistical analysis was performed with a software package (SPSS version 21, Chicago, USA) using an α of 0.05. Mixed-model ANOVA was used to test hypotheses one and two, regarding dependent variables P_{peak} and contact profile components. FSP was treated as a repeated measure, and sex and STT-group as between-subjects factors. When Mauchly's test indicated violations of sphericity for repeated measures, a Greenhouse-Geisser adjustment was employed. A Bonferroni correction was used for STT-group pairwise comparisons to correct for multiple comparisons. Finally, Pearson Product-Moment Correlation (one-tailed) was used to assess the correlation between ellipse descriptors and P_{peak} for hypothesis three.

RESULTS

No pressure or contact profile variable differed significantly between males and females (Table 2).

Table 2: Main effects of sex

Hypothesis	Dependent Variable	F	p
1	P_{peak}	0.293	0.592
2a	*CA*	1.963	0.169
	Eccentricity	3.323	0.076
	H0	2.253	0.142
	H1	0.698	0.410
	H2	1.810	0.187
	H3	3.558	0.067
	H4	0.032	0.858
	H5	0.911	0.346
	HN1	0.028	0.869
	HN2	1.571	0.218
	HN3	3.742	0.061
	HN4	0.000	0.993
	HN5	0.717	0.402

Regarding hypothesis 1, P_{peak} ranged from 307-9992 kPa, and was 29.2% greater during Kneeling Release than Pelvis Release, 71.7% greater during Squat Release than Kneeling Release, and 122.0% greater during Squat Release than Pelvis Release, but not different between STT groups (Table 3, Figure 3).

Table 3: Main effects and significant pairwise comparisons for Hypothesis 1

Dependent Variable	Factor	Pair	F	t	p
P_{peak}	STT		1.179		0.318
	FSP		10.097		0.000**
		Kneeling vs. Pelvis		2.3	0.028*
		Squat vs. Kneeling		2.7	0.010*
		Squat vs. Pelvis		3.8	0.001**

* significant, p<0.05; ** significant, p<0.01

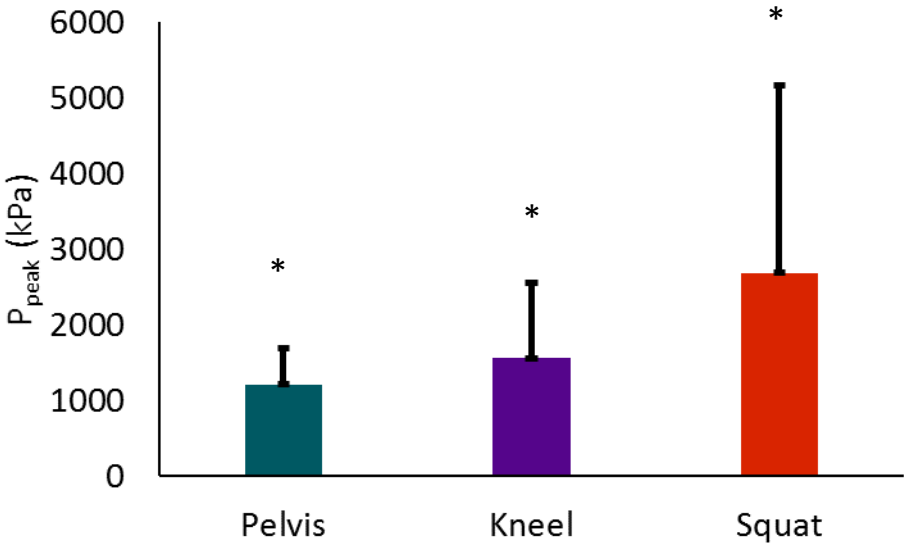

Figure 3: P_{peak} for all participants between FSP * all significantly different, p<0.05.

Regarding hypothesis 2a, *CA* and *H0* differed substantially between STT groups (Table 4, Figure 4a,c); in post hoc comparison, *CA* and *H0* were lower only for low-STT fallers. *CA* and *H0* were lower during Pelvis Release compared to Squat or Kneeling Release (Table 4, Figure 4b,d).

Table 4: Main effects and significant pairwise comparisons for Hypothesis 2a

Dependent Variable	Factor	Pair	F	t	p
CA	STT		8.892		0.001**
		Low vs. medium		-2.7	0.010*
		Low vs. high		-4.2	<0.001**
	FSP		3.9		0.025*
		Pelvis vs. Kneeling		-2.2	0.033*
		Pelvis vs. Squat		-2.4	0.020*
H0	STT		8.52		0.001**
		Low vs. medium		-3.5	0.001**
		Low vs. high		-4.0	<0.001**
	FSP		9.9		<0.001**
		Pelvis vs. Kneeling		-2.4	0.020*
		Pelvis vs. Squat		11.1	<0.001**

*significant, p<0.05; ** significant, p<0.01

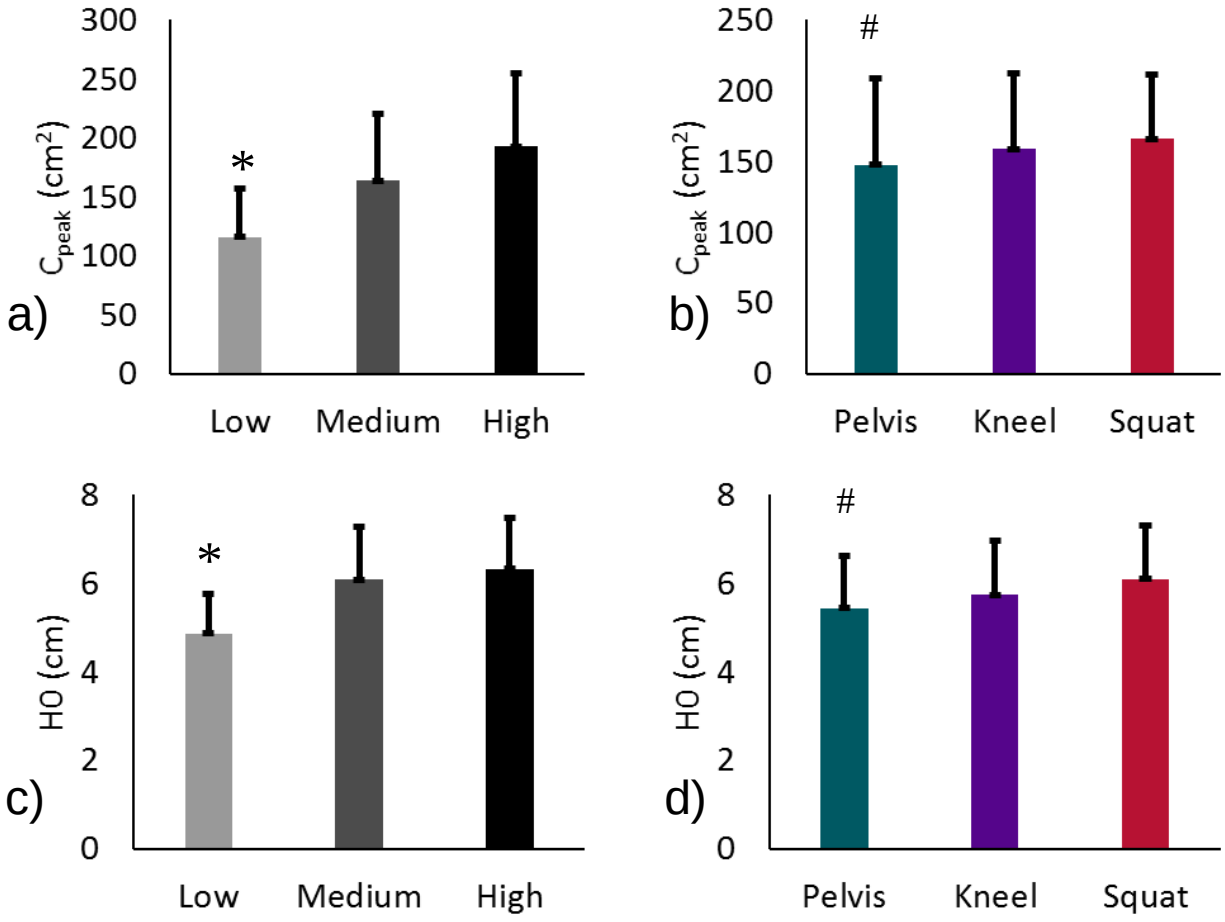

Figure 4: *H0* amplitude (solid) and CA_{peak} between STT groups (a,c) and FSP (b,d) Significant differences, p<0.05: * Low-STT compared to Medium- and High-STT participants; # Pelvis Release compared to Kneeling or Squat Release.

Regarding hypothesis 2b, eccentricity did not differ between FSP, or STT groups; 76.1% of trials resulted in contact profiles with eccentricity greater than 2.0. Interactions between FSP, STT and harmonics were primarily ordinal, and statistical results did not differ substantially between absolute and normalized harmonics. Additionally, the average amplitude of *H3-H5* did not exceed 1 cm, and did not exceed 0.2 of the normalized signal power, therefore, the results reported will focus on *H1* and *H2*. Amplitudes of *H1* ranged from 0.41-6.31 cm, while amplitudes of H2 ranged from 0.35-3.95 cm. *H1* only differed between FSP for low-STT participants (Table 5, Figure 5). *H1* for Pelvis Release was 41.9% lower than Kneeling Release and 42.6% lower than Squat Release. *H2* differed between FSP (Table 5, Figure 5), but trends differed between STT groups. For medium and high-STT groups, *H2* values averaged 35.0% lower for Squat Release compared to Kneeling Release, and 45.4% lower compared to Pelvis Release. *H2* was 61.6% greater during Kneeling Release than Pelvis Release, and 75.6% greater than Squat Release for low-STT participants.

Table 5: Main effects and significant pairwise comparisons for Hypothesis 2b

Dependent Variable	**Factor**	**Pair**	**F**	**t**	**p**
Eccentricity	STT		1.8		0.186
	FSP		1.5		0.239
H1	STT		1.9		0.157
	FSP		8.7		<0.001**
	FSP-STT interaction		3.7		0.008**
	FSP-low STT		12.6		<0.001**
		Pelvis vs. Kneeling		-4.0	0.001**
		Pelvis vs. Squat		-4.1	0.001**
	FSP-medium STT		1.5		0.232
	FSP-high STT		1.8		0.324
H2	STT		0.4		0.657
	FSP		24.5		<0.001**
	FSP-STT interaction		4.9		0.002**
	FSP-low STT		19.6		<0.001**
		Kneeling vs. Pelvis		4.2	0.001**
		Kneeling vs. Squat		5.16	<0.001**
	FSP-medium STT		12.3		<0.001**
		Squat vs. Pelvis		-3.8	0.002**
		Squat vs. Kneeling		-3.7	0.003**
	FSP-high STT		6.6		0.005**
		Squat vs. Pelvis		-3.1	0.015*
		Squat vs. Kneeling		-2.8	0.010*

* significant, $p<0.05$; ** significant, $p<0.01$

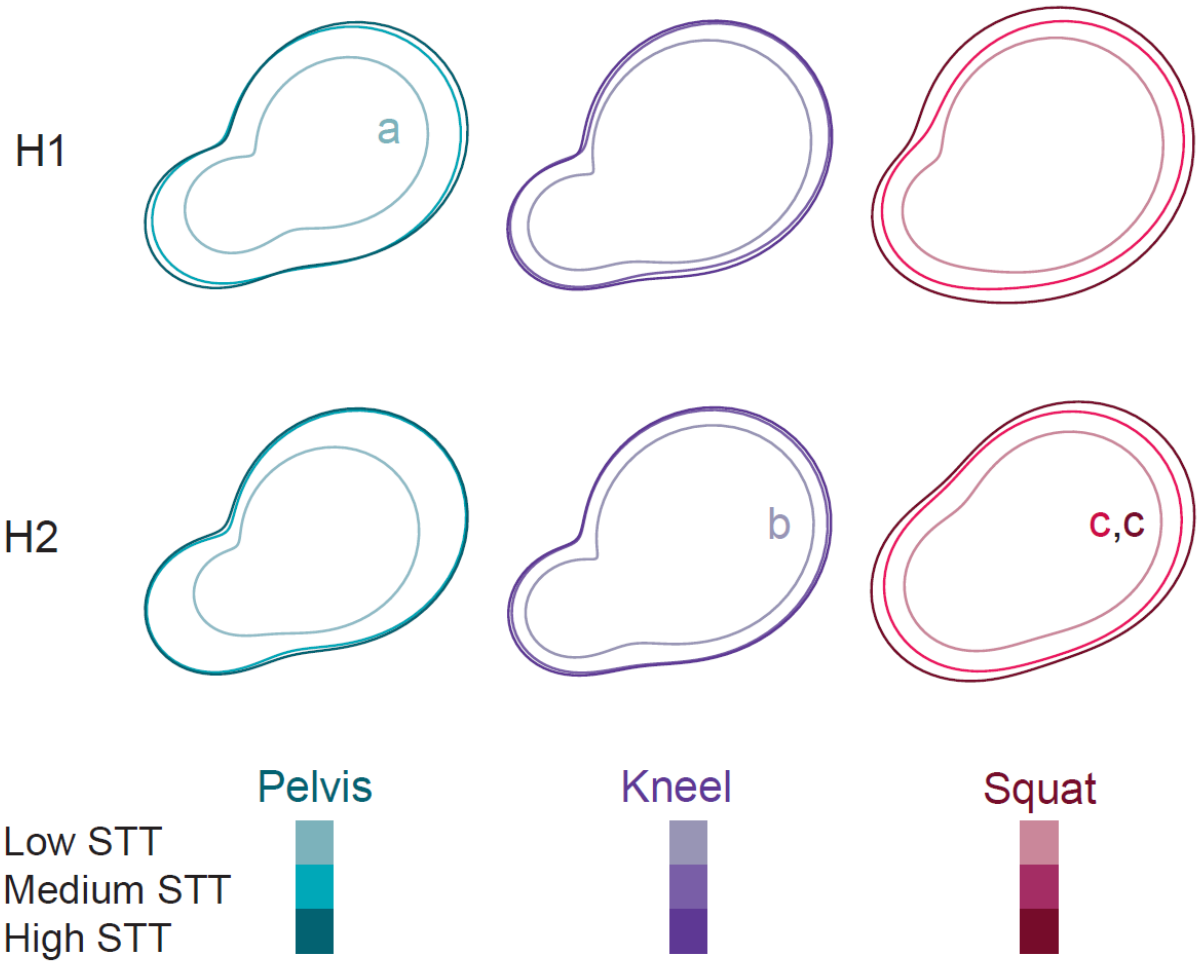

Figure 5: Demonstrated manipulation of H1 and H2 between FSP and STT groups. The top row demonstrates mean FSP contact profiles with H1 manipulated to highlight STT-group differences; the second row demonstrates manipulation of H2 between STT groups.
Significant differences $p<0.05$: a, Pelvis Release lower than Kneeling or Squat Release for low-STT participants; b, Kneeling Release greater than Pelvis or Squat Release for low-STT participants, c, Squat Release lower than Pelvis or Squat Release for medium and high-STT participants.

No contact profile elements were correlated with P_{peak} during Kneeling or Squat Release. P_{peak} was negatively correlated with *CA* and H0…H5 ($p<0.05$), but not eccentricity during Pelvis Release (Figure 6).

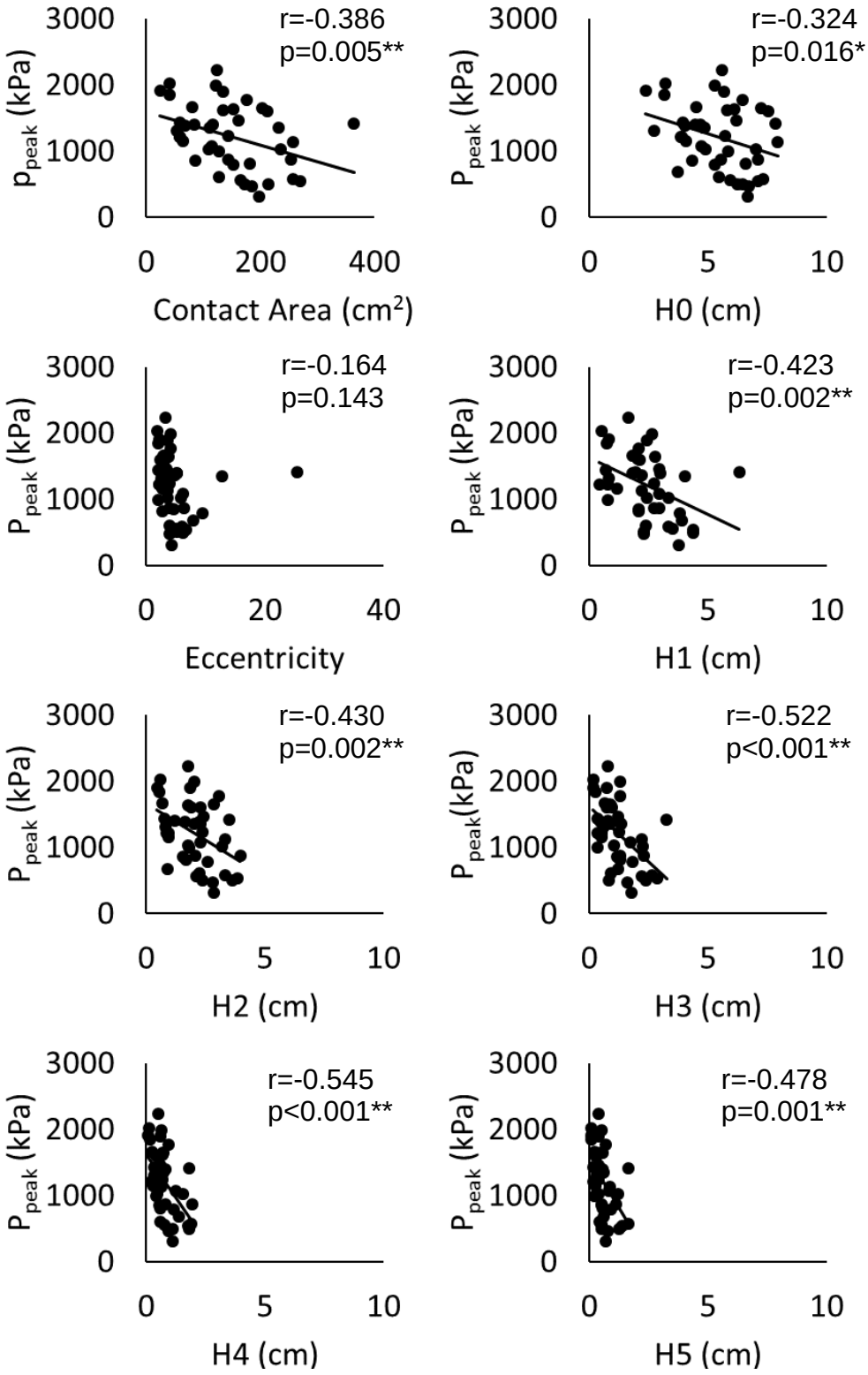

Figure 6: Significant correlations between *M*, *H0…H5* and P_{peak} during Pelvis Release. * significant, p<0.05; ** significant, p<0.01.

DISCUSSION

The goal of this study was to determine how load distribution differed between three fall simulation protocols in male and female participants who exhibited a range of trochanteric soft tissue thickness. Regarding hypothesis one, we found that Peak Pressure was greatest during Squat Release, wherease we predicted that greater Peak Pressure would be observed in protocols with less hip flexion. Additionally, we did not find any difference in Peak Pressure between sex or STT groups. Regarding hypothesis two, we found no difference in Contact Area or *H0* between males and females; however, we found that Contact Area was 35.1% lower, and *H0* was 21.4% lower for low-STT fallers compared to medium- or high-STT participants. Furthermore, we found that Contact Area and *H0* during Pelvis Release were 7.1% and 5.25% lower than Kneeling Release, and 11.0% and 10.8% lower than Squat Release. While we found no difference in Eccentricity between fall simulation protocols, sex or STT groups, harmonic analysis was more sensitive to STT and FSP. Harmonic differences were clearest for low-STT participants, however *H2* also differed between fall simulation protocols for all STT groups. Regarding hypothesis three, we found significant negative correlations between Contact area, *H0-H5* and Peak Pressure only in the Pelvis Release trials.

We did not find differences in P_{peak} or *CA* between males and females, despite a 28.7% decrease in STT for males compared to females. Post hoc analysis of the distribution for P_{peak} revealed that, while 90% of mean FSP outcomes had P_{peak} below 4461 kPa, ten Squat Release trial means (five males, five females) and two Kneeling Release trial means (both female) had P_{peak} values exceeding this boundary. P_{peak} was consistent between the trials comprising each mean. These extreme cases may highlight more critical structural skeletal features than sex differences for P_{peak}. Hip axis length, the distance from the lateral surface of the greater trochanter to the medial surface of the pelvic brim, has been identified as a predictor of hip fracture (Broy, 2015). While we did not measure this component, longer hip axes would, hypothetically, project the greater trochanter further from the pelvis and isolate loading in the "danger zone"; this might explain increased P_{peak} for the extreme cases. The relevance of hip axis length may be counteracted in some cases by STT. We recruited participants with a wide range of STT, and consequently BMI; the effect of these components on the energy of the system has a greater effect than any sex differences. The ratio of hip axis length, or hip projection, to STT may explain outliers in this study, and represents an area of further research.

Further, while P_{peak} during Pelvis Release was similar to those previously reported (Choi, 2010a),P_{peak} and CA did not differ between our STT groups, in contrast to a 266% increase in P_{peak} for low-BMI compared to high-BMI participants reported by Choi et al. The combined effect of mass and STT associated with BMI may have a greater effect on load distribution than STT alone. This is confirmed in our data – when categorized by BMI, we found that P_{peak} was 55.4% higher for low-BMI compared to high-BMI participants (outliers excluded, $t=2.2$, $p=0.038$). *H0-H5* correlated negatively with P_{peak}, and differed between STT groups. Accordingly, there is likely a mechanistic relationship between soft tissue distribution of loads and peak pressure that is not captured by STT. Three-dimensional characterization of trochanteric soft tissue may more effectively highlight group differences.

P_{peak} was substantially greater during Squat Release than Kneeling Release or Pelvis Release, despite having flexion and adduction angles associated with greater apparent STT (Levine, 2014), moderate peak forces and contact area. However, visual analysis of videos of each trial revealed that most participants rotated backwards during the Squat Release protocol; the greater trochanter may project further from the pelvis in the posterolateral rather than lateral aspect. Posterolateral impact configurations have previously been linked with greater peak pressure, particularly for low-BMI fallers (Choi, 2010a).

Harmonic analysis was more sensitive to FSP-STT interactions than eccentricity, and more strongly correlated with P_{peak}. Amplitudes of *H3-5* were low, and, on average, represented 17.9% of the signal power. However, all six harmonics investigated were negatively correlated with P_{peak} for pelvis release. The link between *H3-5* and P_{peak} is likely due to the interdependence and phase angle of the harmonics. The contact profile is composed of interfering waves, and no harmonic can independently characterize the shape. Interference of the waveforms associated with higher-order harmonics may emphasize aspects of lower-order harmonics (*H0-H2*) rather than influencing independent semilandmarks. Analysis of phase angles would clarify this effect. Higher-order harmonics may have greater utility for contact profiles with higher frequency content, e.g. an impact to an outstretched hand. However, Radial Fourier Analysis is only appropriate for closed curves, and each radius must cross the contact outline only once; other morphometric methods, such as more complex Fourier shape signatures (El-ghazal, 2009) or eigenshape functions (Lohmann, 1983) may be more appropriate.

The results of this study have implications for prediction of, and intervention to prevent hip fracture. First, we found that the Squat Release protocol produced substantially greater P_{peak} than the other fall simulation methods, despite moderate peak forces and contact area. This protocol may represent a "high risk" impact configuration; further work should quantify what interactions of anatomy, faller behavior and impact mechanics are responsible for the increase in P_{peak}. Second, we found that all FSP and participants produced substantial *H1* components, which points towards a circular contact profile as suitable for modeling of impacts to the hip. However, further work should assess the sensitivity of models to the influence of higher-order harmonics, and set *a priori* harmonic thresholds. Third, we found limited differences between results of absolute and normalized harmonics, in addition to, and likely due to, ordinal interactions between STT group, FSP and the harmonics. This points towards the scalability of contact profiles based on body composition, a simplification in creating individual-specific injury prediction models. Finally, *H0* was negatively correlated with P_{peak} for Pelvis Release, which suggests that distribution of loads away from the "danger zone" may be of similar importance as energy absorption in reducing peak pressure. Therefore, wearable or environmental interventions to prevent hip fracture, such as hip protectors or safety floors, could be designed to reflect this—a thinner product with better load distribution performance may be more effective than current bulky models. This hypothesis already has support in the case of horseshoe vs. continuous hip protectors (Laing, 2011; Laing and Robinovitch, 2008).

CONCLUSIONS

In this study, we quantified P_{peak} and *CA* differences and interactions between fall simulation method, sex and STT groups using morphometric methods. We found that method of falling had the strongest effect on P_{peak}, compared to STT or sex, and substantial effects on several indices of load distribution. Further, we found that STT also had a substantial effect on load distribution. Finally, we found that ellipse descriptors were effective predictors of P_{peak} during some simulated falls.

ACKNOWLEDGEMENTS

This research was funded in part by an operating grant from the Natural Sciences and Engineering Research Council of Canada (grant # 386544), an infrastructure grant from the Canadian Foundation for Innovation, and infrastructure and Early Career Research Award grants from the Ontario Ministry of Research and Innovation.

REFERENCES

BHAN, S., LEVINE, I.C., LAING, A.C., (2014). Energy absorption during impact on the proximal femur is affected by body mass index and flooring surface. J. Biomech. 47, 2391–2397.

BOOS, M., MCPHEE, J., (2013). Volumetric modeling and experimental validation of normal contact dynamic forces. J. Comput. Nonlinear Dyn. 8, 21006-021006-8.

BOUXSEIN, M.L., SZULC, P., MUNOZ, F., THRALL, E., SORNAY-RENDU, E., DELMAS, P.D., (2007). Contribution of Trochanteric Soft Tissues to Fall Force Estimates, the Factor of Risk, and Prediction of Hip Fracture Risk. J. Bone Miner. Res. 22, 825–831.

BROY, S.B., CAULEY, J.A., LEWIECKI, M.E., SCHOUSBOE, J.T., SHEPHERD, J.A., LESLIE, W.D., (2015). Fracture risk prediction by non-BMD DXA measures: the 2015 ISCD official positions part 1: hip geometry. J. Clin. Densitom. 18, 287–308.

CHOI, W.J., HOFFER, J.A., ROBINOVITCH, S.N., (2010a). The effect of positioning on the biomechanical performance of soft shell hip protectors. J. Biomech. 43, 818–825.

CHOI, W.J., HOFFER, J.A., ROBINOVITCH, S.N., (2010b). Effect of hip protectors, falling angle and body mass index on pressure distribution over the hip during simulated falls. Clin. Biomech. 25, 63–69.

CUMMINGS, S.R., NEVITT, M.C., (1994). Non-skeletal determinants of fractures: the potential importance of the mechanics of falls. Osteoporos. Int. 4, S67–S70.

EHRLICH, R., WEINBERG, B., (1970). An exact method for characterization of grain shape. J. Sediment. Res. 40, 205–212.

EL-GHAZAL, A., BASIR, O., BELKASIM, S., (2009). Farthest point distance: A new shape signature for Fourier descriptors. Signal Process. Image Commun. 24, 572–586.

ETHERIDGE, B.S., BEASON, D.P., LOPEZ, R.R., ALONSO, J.E., MCGWIN, G., EBERHARDT, A.W., (2005). Effects of trochanteric soft tissues and bone density on fracture of the female pelvis in experimental side impacts. Ann. Biomed. Eng. 33, 248–254.

GONTHIER, Y., MCPHEE, J., LANGE, C., PIEDBŒUF, J.-C., (2005). A contact modeling method based on volumetric properties, ASME 2005 International Design Engineering

Technical Conferences and Computers and Information in Engineering Conference. American Society of Mechanical Engineers, 477–486.
HAYES, W.C., MYERS, E.R., ROBINOVITCH, S.N., VAN DEN KROONENBERG, A., COURTNEY, A.C., MCMAHON, T.A., (1996). Etiology and prevention of age-related hip fractures. Bone 18, S77–S86.
JOHANSSON, H., KANIS, J.A., ODÉN, A., MCCLOSKEY, E., CHAPURLAT, R.D., CHRISTIANSEN, C., CUMMINGS, S.R., DIEZ-PEREZ, A., EISMAN, J.A., FUJIWARA, S., GLÜER, C.-C., GOLTZMAN, D., HANS, D., KHAW, K.-T., KRIEG, M.-A., KRÖGER, H., LACROIX, A.Z., LAU, E., LESLIE, W.D., MELLSTRÖM, D., MELTON, L.J., O'NEILL, T.W., PASCO, J.A., PRIOR, J.C., REID, D.M., RIVADENEIRA, F., VAN STAA, T., YOSHIMURA, N., ZILLIKENS, M.C., (2014). A Meta-Analysis of the Association of Fracture Risk and Body Mass Index in Women. J. Bone Miner. Res. 29, 223–233.
LAING, A.C., FELDMAN, F., JALILI, M., TSAI, C.M., ROBINOVITCH, S.N., (2011). The effects of pad geometry and material properties on the biomechanical effectiveness of 26 commercially available hip protectors. J Biomech 44, 2627–2635.
LAING, A.C., ROBINOVITCH, S.N., (2008). Effect of soft shell hip protectors on pressure distribution to the hip during sideways falls. Osteoporos. Int. 19, 1067–1075.
LAING, A.C., TOOTOONCHI, I., HULME, P.A., ROBINOVITCH, S.N., (2006). Effect of compliant flooring on impact force during falls on the hip. J. Orthop. Res. 24, 1405–1411.
LEVINE, I.C., BHAN, S., LAING, A.C., (2013). The effects of body mass index and sex on impact force and effective pelvic stiffness during simulated lateral falls. Clin. Biomech. 28, 1026–1033.
LEVINE, I.C., MINTY, L.E., LAING, A.C., (2014). Factors that influence soft tissue thickness over the greater trochanter: Application to understanding hip fractures. Clin. Anat. 28, 253–261.
LOHMANN, G.P., (1983). Eigenshape analysis of microfossils: A general morphometric procedure for describing changes in shape. J. Int. Assoc. Math. Geol. 15, 659–672.
NIELSON, C.M., BOUXSEIN, M.L., FREITAS, S.S., ENSRUD, K.E., ORWOLL, E.S., (2009). Trochanteric soft tissue thickness and hip fracture in older men. J. Clin. Endocrinol. Metab. 94, 491-496.
ROBINOVITCH, S.N., EVANS, S.L., MINNS, J., LAING, A.C., KANNUS, P., CRIPTON, P.A., DERLER, S., BIRGE, S.J., PLANT, D., CAMERON, I.D., KIEL, S.P., HOWLAND, J., KHAN, K., LAURITZEN, J.B., (2009). Hip Protectors: Recommendations for Biomechanical Testing – an International Consensus Statement (part I). Osteop Int 20, 1977–1988.
ROBINOVITCH, S.N., HAYES, W.C., MCMAHON, T.A., (1995a). Energy-shunting hip padding system attenuates femoral impact force in a simulated fall. J. Biomech. Eng. 117, 409–413.
ROBINOVITCH, S.N., HAYES, W.C., MCMAHON, T.A., (1991). Prediction of femoral impact forces in falls on the hip. J. Biomech. Eng. 113, 366-374.
ROBINOVITCH, S.N., MCMAHON, T.A., HAYES, W.C., (1995b). Force attenuation in trochanteric soft tissues during impact from a fall. J. Orthop. Res. 13, 956–962.